Electronic Supplementary Material (ESI) for Journal of Materials Chemistry C
This journal is © The Royal Society of Chemistry 2014

Supporting Information

Highly stable solution-processed ZnO thin film transistors via simple Al evaporation process

*By Tae Sung Kang, Tae Yoon Kim, Gyu Min Lee, Hyun Chul Sohn, and Jin Pyo Hong**

1. Possible geometric layouts of Al-evaporated ZnO TFTs at short and long deposition times

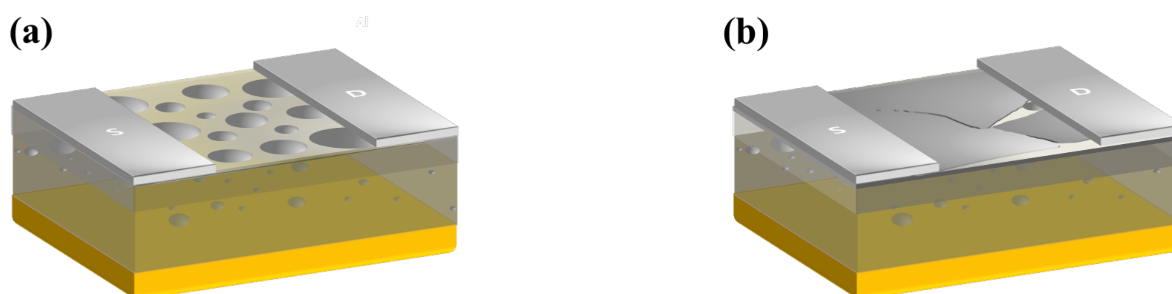

Fig. S1 Possible illustrations of Al-evaporated ZnO TFT prepared at (a) a short deposition time of 40 sec and (b) a long deposition time of 50 sec.

Fig. S1a and S1b reveal possible schematics of bottom gate solution-deposited ZnO TFTs evaporated by Al on the surface channel layer at two different deposition times of 40 sec and 50 sec, respectively. The ZnO and Al NPs were fabricated at room temperature. In particular, the deposition time of the Al was carefully controlled for the appearance of Al NPs on the back channel. In our work, the formation of Al nanoparticles (NPs) seemed to occur at a short deposition time (40 sec), covering the whole ZnO channel layer. After that, the same Al source/drain electrodes were thermally evaporated. However, as shown in Fig. S1b, an Al metal thin film appeared at a relatively long Al deposition time (50 sec), confirming large leakage current paths between the source and drain.

2. I-V curves of pure ZnO and Al-evaporated ZnO TFTs at various deposition times

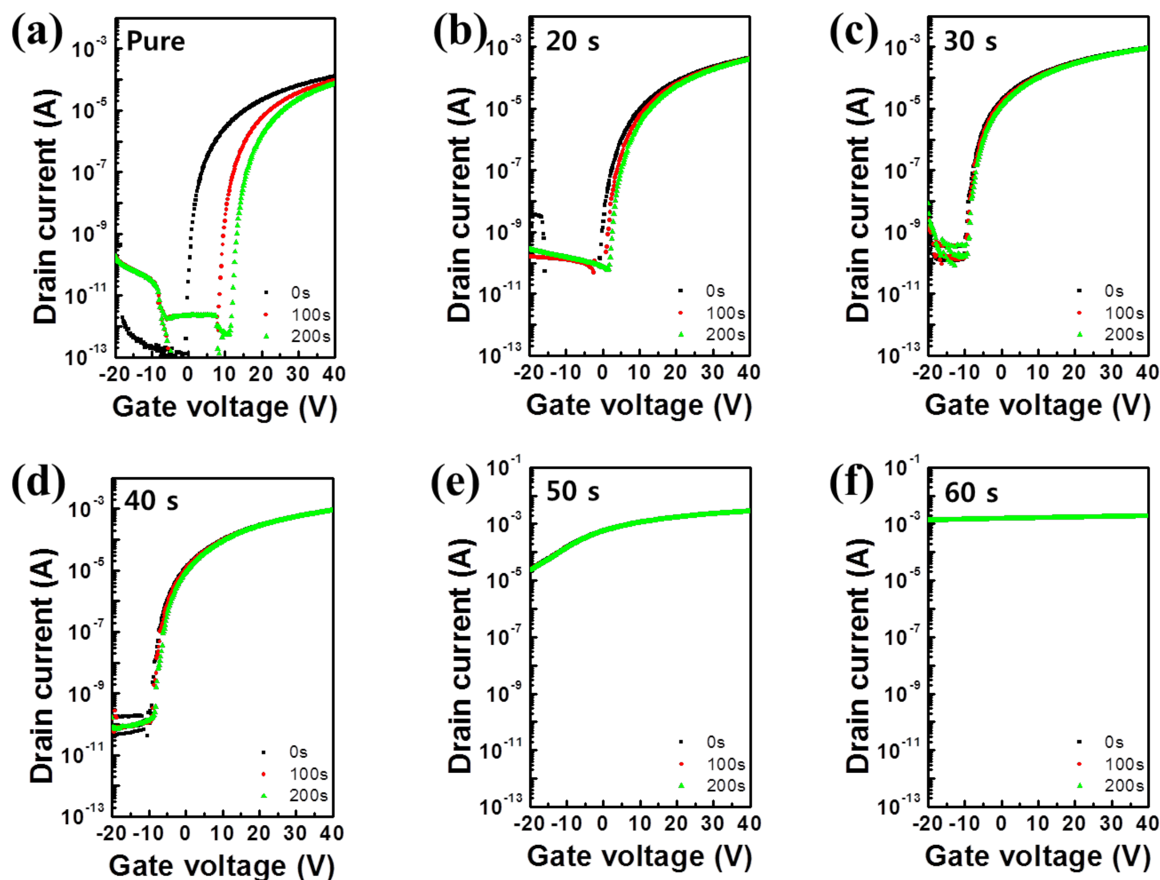

Fig. S2 Typical transfer curves (I_{ds}-V_{gs}) of pure ZnO and Al-evaporated ZnO TFTs as a function of deposition time: (a) pure, (b) 20 s, (c) 30 s, (d) 40 s, (e) 50 s and, (f) 60 s (V_{ds} = +10 V, V_{gs} = from -20 to 40 V) deposited samples. The pure ZnO TFT revealed the threshold voltage shift after applying a gate bias of 20 V for 200 s, while the proper deposition of Al on the back channel of ZnO provided relatively stable electric responses. However, the I-V characteristics of Al-evaporated ZnO TFTs prepared at a long deposition time of 50 sec were clearly deteriorated, demonstrating the formation of Al metal film on the back channel of ZnO layer, not the appearance of Al NPs.

3. Cross-sectional STEM image of Al-evaporated ZnO TFT

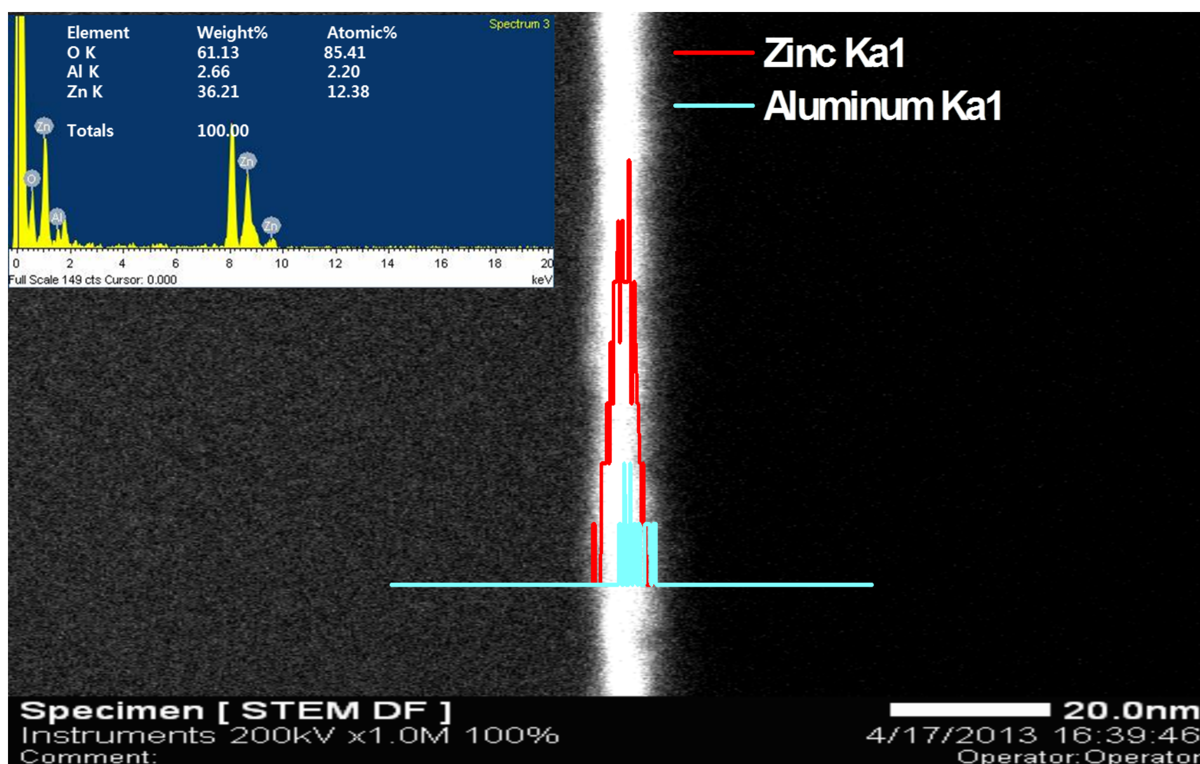

Fig. S3 Cross-sectional STEM image of an Al-evaporated ZnO TFT, displaying the atomic depth-profiles of Zn and Al. The inset of the figure reveals energy dispersive X-ray spectroscopy.

4. Electron accumulation induced by forming hetero interface at ZnO/AlZnO.

The figure described below indicates the possible energy band schematic of ZnO/AlZnO heterojunction system

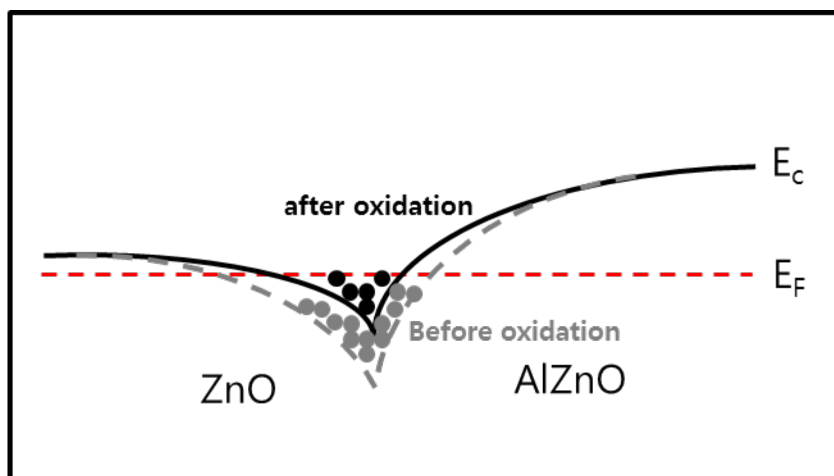

Fig. S4 The schematic of ZnO/AlZnO heterojunction, exhibiting electron accumulation at the hetero interface. Energy well was decreased after the oxidation of Al due to the thermal equilibrium betweem Al and AlZnO.

This journal is © The Royal Society of Chemistry 2014

5. SIMS depth profiles

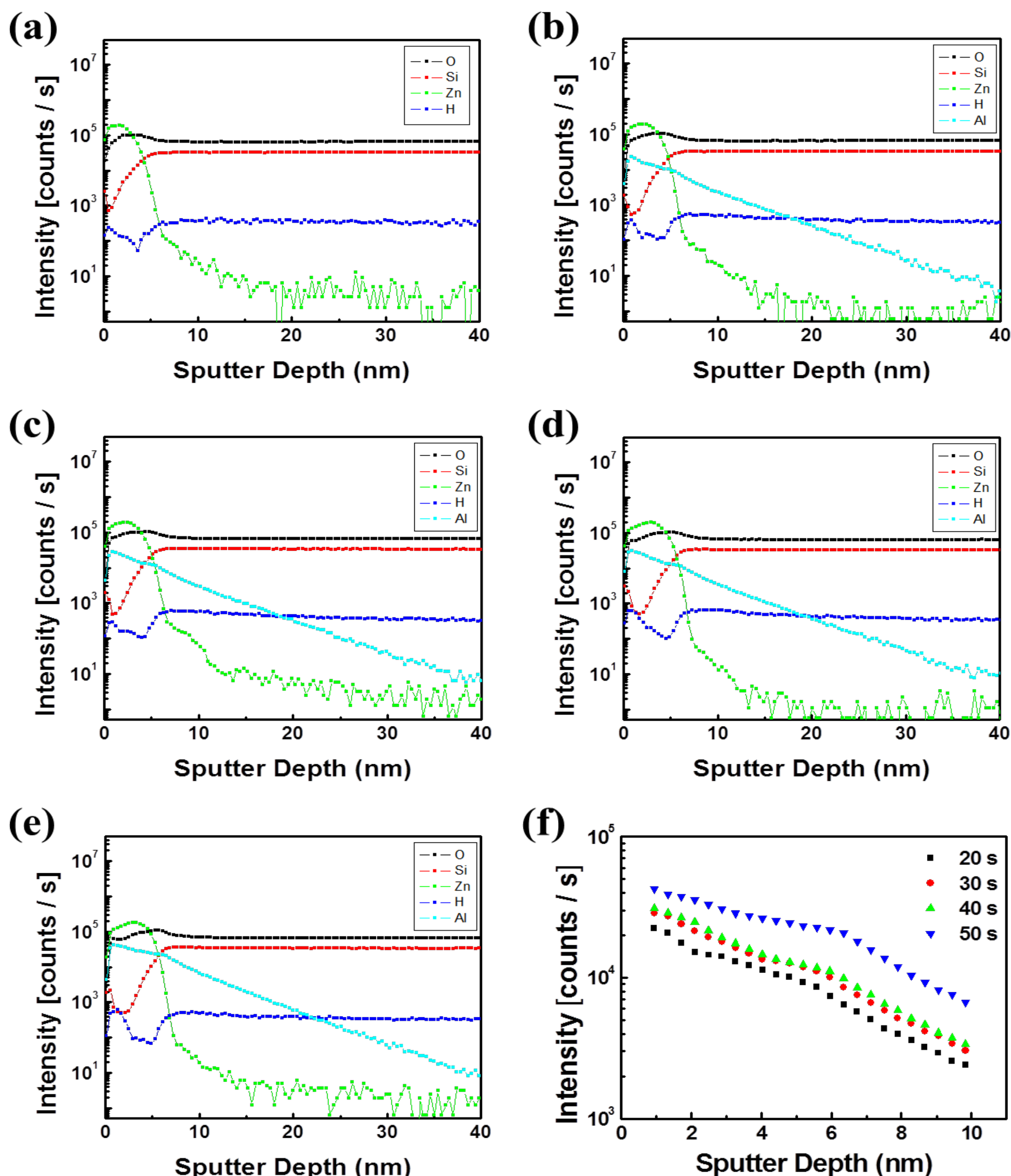

Fig. S5 SIMS depth profile of (a) pure ZnO and Al-evaporated ZnO TFTs at (b) 20 s, (c) 30 s, (d) 40 s , (e) 50 s, and (f) existence of the impregnated Al atoms or ions inside the ZnO layer, depending on Al deposition time.

Fig. S5 presents the SIMS depth profiles of pure ZnO and Al-evaporated ZnO TFTs at various Al deposition times ranging from 0 to 50 s, indicating that the impregnated Al atoms or ions increased with increasing deposition time. Inhomogeneous signals of Al atoms were detected underneath the Al-evaporated ZnO layer, owing to unintended re-deposition of Al atoms during secondary ion beam sputtering. In addition, an unstable transient region can occur at the onset of system operation such that the sputtered ions were increased rapidly for the first few seconds.

6. Threshold voltage shifts of pure ZnO and Al-evaporated ZnO TFTs under stress

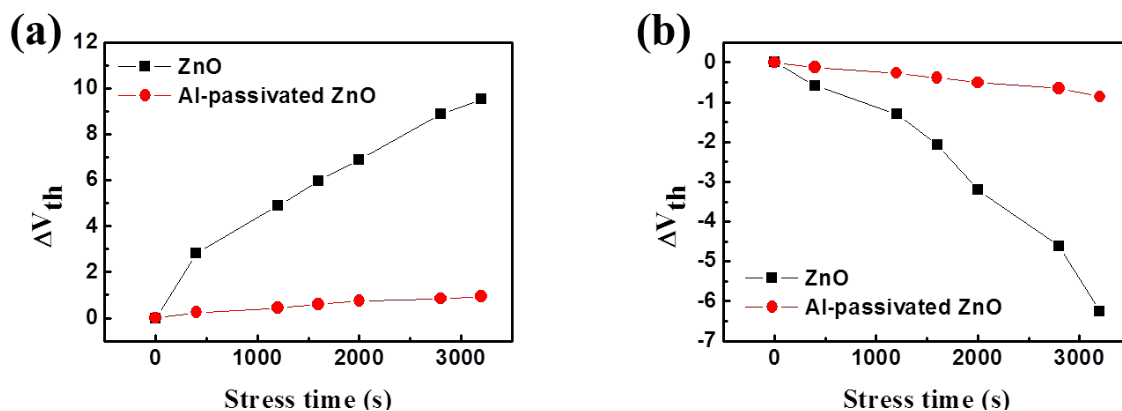

Fig. S6 Relative threshold voltage shift of pure ZnO (black squares) and Al-evaporated ZnO TFTs (red circles) in the (a) positive and (b) negative directions as a function of stress time. The Al-evaporated ZnO TFT revealed relatively stable features, as expected.